PREDICTION OF THE MANOEUVRING BEHAVIOUR OF THE KCS BASED ON RANS-SIMULATED CAPTIVE TESTS

Andrés Cura-Hochbaum and Sebastian Uharek
TU Berlin, Germany

SUMMARY

Given rudder manoeuvres are simulated for the KRISO container ship (KCS) sailing in deep and shallow water using a mathematical model of Abkowitz type. The necessary hydrodynamic coefficients are determined by means of static and dynamic virtual PMM tests performed with the RANS code Neptuno developed by the authors. The effect of the propeller is modelled with a body force model.

1 INTRODUCTION

A widely used method to simulate rudder manoeuvres of a ship is to obtain a set of hydrodynamic coefficients from captive model tests with prescribed motions and use it to solve the motion equations of the ship. All dynamic captive tests were done with a virtual CPMC. The main advantage of a virtual CPMC over a virtual PMM is the ability to keep the longitudinal speed of the ship constant by using an additional x-drive. This is especially important for the pure yaw test.

In the present case these model tests are simulated by means of Reynolds-Averaged-Navier-Stokes (RANS) calculations with the code Neptuno. Although it is possible to calculate the hydrodynamic forces and moments acting on the hull in every time step and update the motions of the ship accordingly there are some advantages of a coefficient based approach. A set of hydrodynamic coefficients allows the quick prediction of any manoeuvre - for example a Williamson turn - without any additional time consuming RANS calculations needed.

For the prediction of the free surface viscous flow around the considered ship, the incompressible RANS equation and the continuity equation are solved numerically with a finite volume method on a block structured grid allowing non matching interfaces. Pressure and velocity are coupled with the SIMPLE method. All computations were performed with an updated version of the RANS code Neptuno. This code has been described in [2]. It uses the standard k-ω turbulence model from Wilcox [4]. The free surface is calculated with the level set technique.

After the manoeuvring derivatives are determined using the time histories of the forces and moments gathered from the RANS computations, the motion equations of the ship represented as a rigid body are integrated in four degrees of freedom over time.

Table 1: Main Particulars

	full scale	model
λ	1.000	37.890
L_{PP} [m]	230.0	6.0702
B_{WL} [m]	32.2	0.8498
T [m]	10.8	0.2850
V [m^3]	52030	0.9565
S [m^2] (w/o Rud)	9530	6.6381
Turn rate [deg/s]	2.32	14.3
v [m/s]	12.35	2.005
Fn	0.26	0.26
Re	$2.84 \cdot 10^9$	$1.22 \cdot 10^7$
I_{xx}/B	0.4	0.4
I_{zz}/L_{PP}	0.25	0.25
$\overline{GM}$ [m]	0.6	0.016
$\overline{KM}$ [m]	14.9	0.3932
shallow water		
H/T	1.2	1.2
v [m/s]	4.513	0.733
Fn	0.095	0.095
Re	$1.04 \cdot 10^6$	$4.45 \cdot 10^6$

This procedure has been used to predict the manoeuvrability of the KCS whose main particulars are shown in Table 1. This paper shows how the results handed in to the SIMMAN14 workshop have been calculated.

2 RANS-SIMULATIONS

All calculations were performed for the KCS in model scale (1:37.89). Two grids - the coarse consisting of 462000 cells and the fine with 3.7 million cells - are used for every calculation to estimate the effect of the grid resolution. The deflection of the rudder was implemented using a individual grid box for every rudder angle. For calculating the static heel cases two additional grids were generated. All grids were built with the commercial software ICEM and have non matching block interfaces.

The solutions of all equations are calculated in a non inertial, ship fixed coordinate system. For prescribing the motions in case of a dynamic test the boundary conditions are updated and inertial forces are added to the RANS equations accordingly.

The turbulence is modelled with the Wilcox k-ω model and wall functions have been used. For the CFD calculations all motions were given, the model was not free to sink and trim.

The body force model of the original nepIII code has been modified to use a precalculated database of propeller disk forces for different inflow angles and advance coefficients.

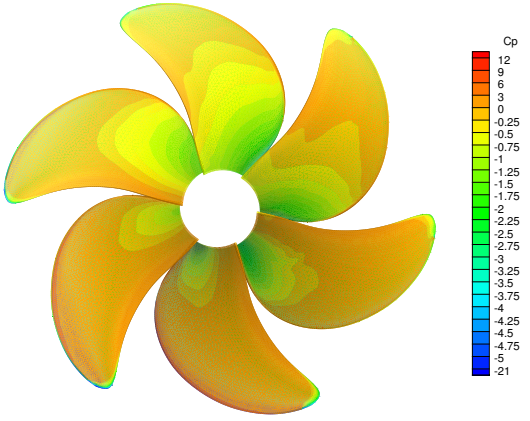

Fig. 1: Precalculated pressure distribution on the used stock propeller (uniform inflow with $\beta = 30°$)

The disk forces are obtained by RANS calculations for the isolated rotating propeller in uniform inflow. (see figure 1)

Since these calculations are very time consuming and the KCS propeller has not been calculated yet, the existing database of a very similar (stock) propeller (see open water diagram in figure 2) was used for the virtual tests. Disregarding the number of blades, all propeller parameters were the same as the KCS. The propeller revolution was chosen at model self propulsion point (MSPP) for all tests, since the results are going to be compared with free manoeuvring tests performed without skin friction correction force.

For all dynamic virtual model tests a motion period of 25 seconds was chosen. The used time step was 1/2500 of the motion period. To achieve the desired convergence in every time step ten SIMPLE iterations were sufficient.

In order to cover a broad band of surge velocities a rather high amplitude of 0.25 made nondimensional with the approach speed was selected for the pure sway test. This is an advantage of the virtual CPMC tests, because there are no restrictions due to physical limitations of the carriage. The other nondimensional velocity amplitudes were: 0.50 for pure sway, 0.70 for pure yaw and -0.4, 0.70 and 0.40, 0.40 for two combined sway-yaw tests, respectively.

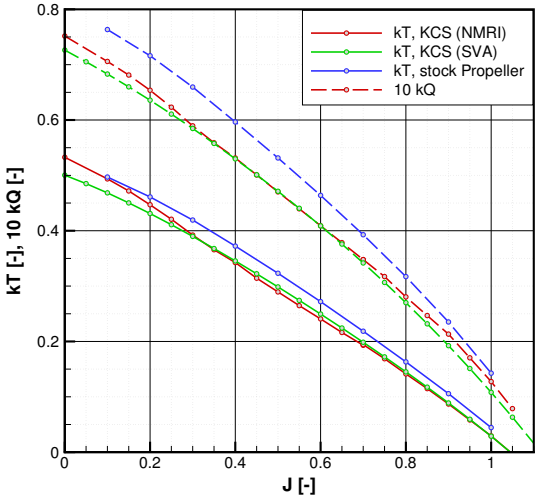

Fig. 2: Comparison of open water diagrams for the KCS and used stock propeller

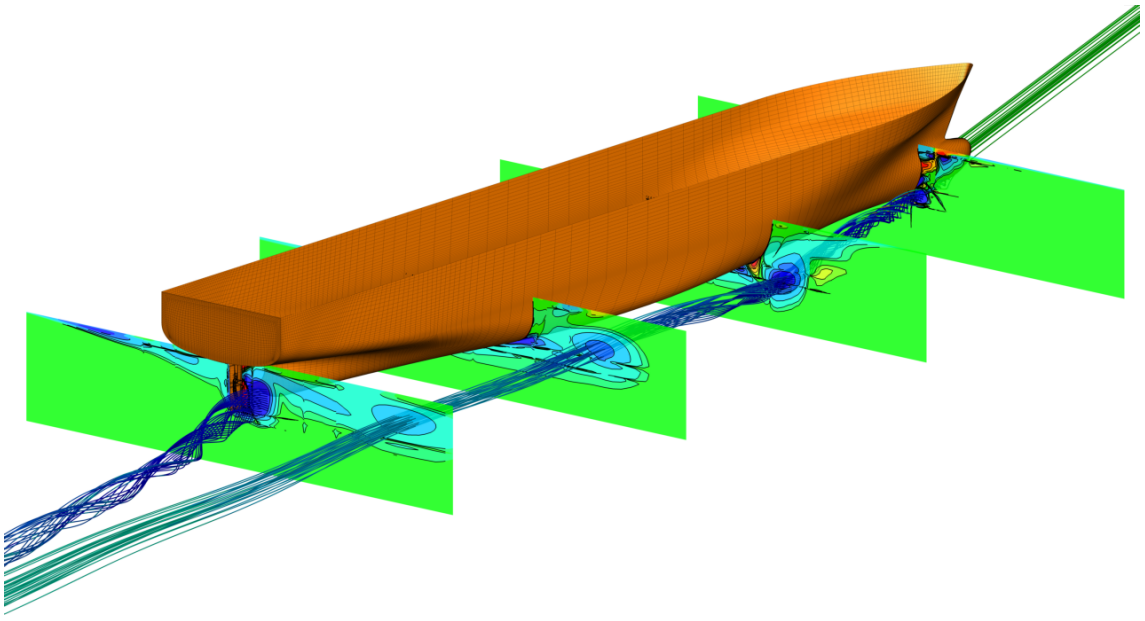

Fig. 3: Vortex generation at leeward side with 20° drift angle (contour shows vorticity)

Figure 4 shows the comparison between the results calculated on the coarse grid and those calculated on the fine grid. Only a small difference for large rudder angles can be detected in side force and yaw moment. This is due to insufficient resolution at the rudder with the coarse grid. As a result the stall is not captured correctly. In figure 6 the different separation behaviour on the coarse and the fine grid is shown. The top pictures show the attached flow at 25° rudder angle for the fine (left) and coarse (right) grid. When the rudder angle reaches 35° (bottom), the flow is separated and the resulting vortex gets underestimated on the coarse grid.

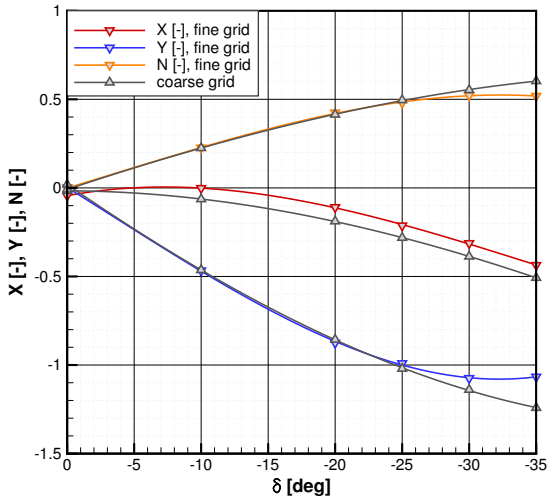

Fig. 4: Rudder deflection test: grid dependency

For these reasons all static tests were done on the fine grid. Because all dynamic tests were performed at zero rudder angle, the time histories are nearly identical (see figure 7). Hence for all dynamic tests the coarse grid with only 462000 cells could be used.

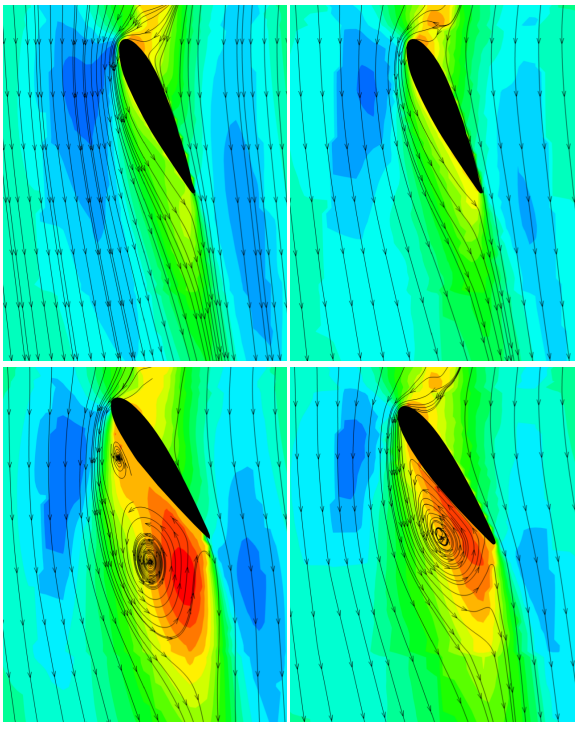

Fig. 6: Separation coarse vs. fine grid

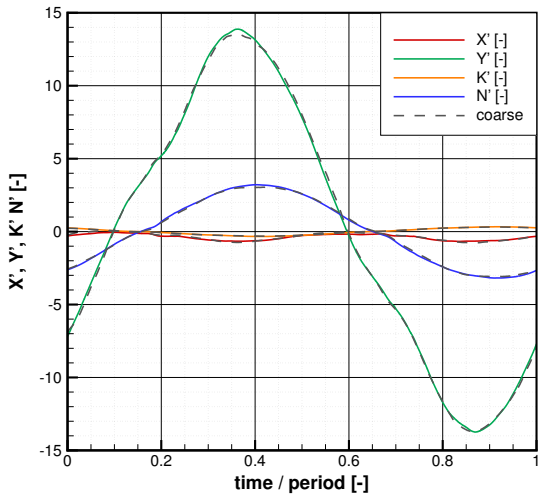

Fig. 7: Time series of nondimensional forces and moments during simulated pure sway test

A total number of 84 virtual tests for each grid resolution have been calculated on a high performance cluster to cover the large matrix of virtual model tests. The average calculation time was 13/180 hrs. (coarse / fine) for the static rudder deflection tests and 30/223 hrs. for one motion period of the simulated dynamic CPMC tests.

For the shallow water case the boundary condition at the bottom has been modified from a slip wall to a uniform prescribed velocity. The free surface elevation of a static drift and static yaw test in deep and shallow water is shown in figure 8.

3 MATHEMATICAL MODEL

The mathematical model used for calculating the hydrodynamic forces acting on the ship in every time step is of Abkowitz type with coefficients up to third order. [1]

The dynamic CPMC tests were analysed by a fourier analysis of the time series. Further a regression analysis of all static tests was performed. The satisfactory quality of the regression can be seen in figure 9 which shows the calculated nondi-

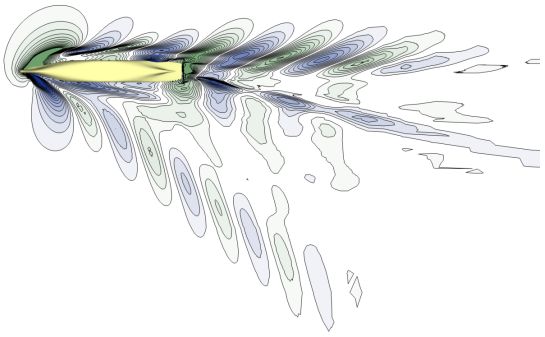

(a) deep water, static drift $\beta = 20°$

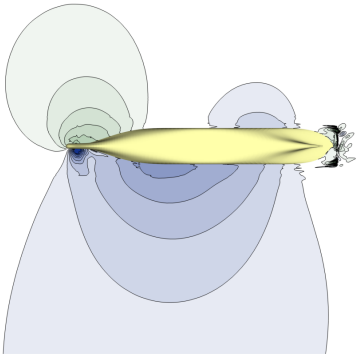

(b) shallow water, static drift $\beta = 10°$

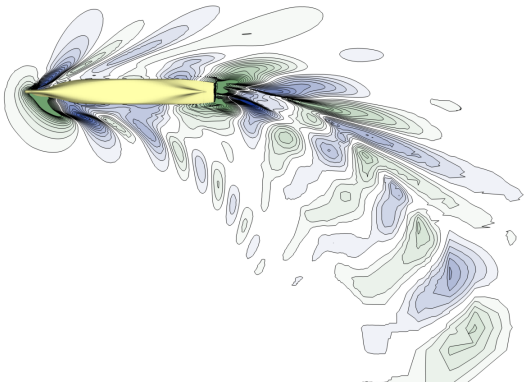

(c) deep water, static yaw $r' = 0.7$

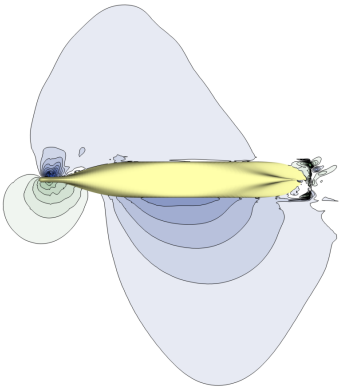

(d) shallow water, static yaw $r' = 0.7$

Fig. 8: Free surface during static tests in deep and shallow water (contour lines not at same levels)

mensional yaw moment during static drift tests (symbols) at various rudder angles and the reconstructed values using the hydrodynamic coefficients (lines).

All forces have been made nondimensional with respect to water density, longitudinal ship speed and length.

The results of the virtual tests in heeled condition up to 8° show that the dependency of the X' and Y' force and the N' and K' moment on heel angle is rather small in this case. Thus this effect was neglected in the mathematical model. The roll damping coefficient has been taken from forced roll experiments with a similar ship.

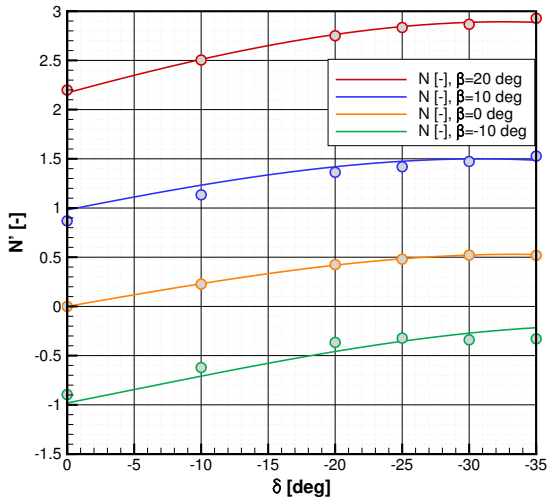

Fig. 9: Example of regression quality check

4 MANOEUVRE SIMULATIONS

For predicting rudder manoeuvres the motion equations of the ship represented as a rigid body are integrated in time. All manoeuvring simulations have been performed for the model at MSPP as required by the organizers. The results however are written for the full scale ship. though MSPP was chosen for all calculations, the manoeuvring simulations were performed for the full scale ship. The time integration was performed by a first order explicit Euler method. As mentioned before the dependency on heel angle was not included in the mathematical model, but nevertheless the simulations were performed taking four degrees of freedom into account.

The simulated turning circle in deep water (figure 10) shows an advance of 3.04 L_{PP}, a tactical diameter of 2.73 L_{PP} and a steady turning diameter of 2.33 L_{PP}. Therefore the KCS fulfils all IMO requirements regarding turning circle tests with margins. [3]

The results of the 10°/10° zigzag test starting to starboard are shown in figure 11. The first overshoot angle is 7.4 deg, the second 12.5 deg. These values are inside the IMO limits as well.

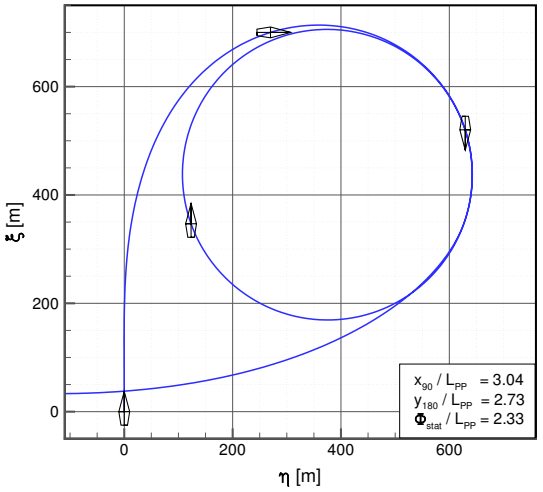

Fig. 10: Simulation of a turning circle with $\delta = 35°$ and pull-out in deep water

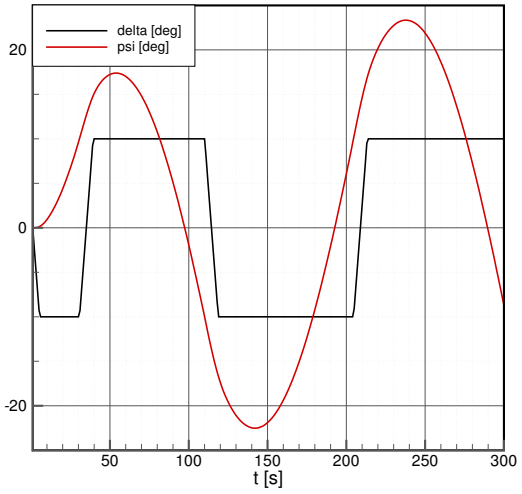

Fig. 11: Simulated 10°/10° zigzag test starting to starboard in shallow

In shallow water the advance increases to 4.78 L_{PP} and the tactical diameter is 7.14 L_{PP}. The steady turning diameter is 5.91 L_{PP}. The results of the 10/2.5° zigzag test is shown in figure 13.

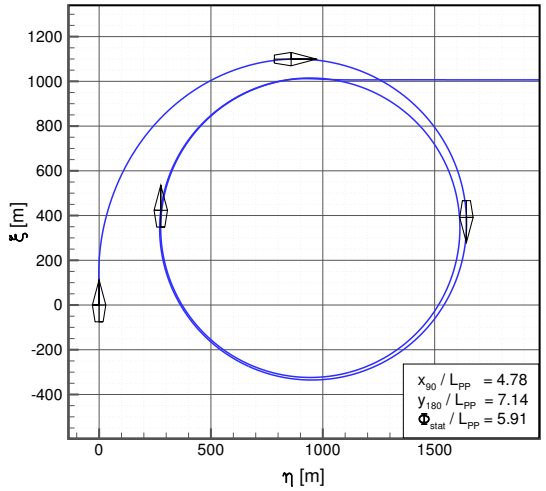

Fig. 12: Simulation of a turning circle with $\delta = 35°$ and pull-out in shallow water

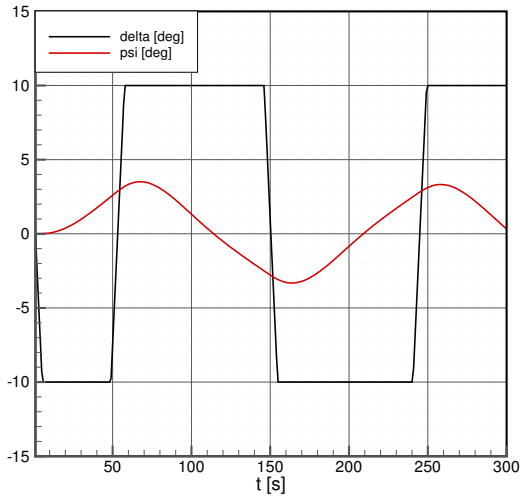

Fig. 13: Simulated $10°/2.5°$ zigzag test starting to starboard in shallow water

5 CONCLUSIONS

Standard rudder manoeuvres have been simulated successfully by means of a mathematical model of Abkowitz type. The hydrodynamic coefficients were purely determined by means of virtual model tests performed with the RANS code Neptuno. The results of the turning circle and zigzag test fulfil all IMO recommendations with margin. It can be noted that for all situations that do not involve high effective rudder angles and therefore stall a coarse grid with less than 500.000 cells shows nearly identical results as a fine grid with over 3.5 million cells.

The dependency on the heel angle seems to be smaller than expected in this case and had only very limited influence on the results of the simulated manoeuvres.

REFERENCES

[1] M A Abkowitz. Lectures on Ship Hydrodynamics–Steering and Manoeuvrability, 1964.

[2] Andrés Cura Hochbaum and M Vogt. Towards the simulation of seakeeping and maneuvering based computation of the free surface viscous ship flow. *24th ONR Symp. on Naval Hydrodynamics, Fukuoka*, 2002.

[3] International Maritime Organization. Resolution MSC.137(76), Standards for Ship Manoeuvrability. *London*, 2002.

[4] David C. Wilcox. *Turbulence Modeling for CFD (1st edition)*. DCW Industries, 1993.